 https://doi.org/10.24191/jeesr.v29i1.007

Design and Experimental Validation of a Class-E LCCL Capacitive Power Transfer System for Low-Power Wireless Charging Applications

Muhammad Izzat Ariff Bin Sulaiman, Khairul Kamarudin Bin Hasan*, Nor Diyana Binti Md Sin, Zakariah Bin Yusuf, and Siti Aminah Nordin

***Abstract*—Capacitive power transfer (CPT) offers a lightweight and metal-tolerant alternative to inductive wireless power transfer for short-range, low-power charging applications. This paper presents a Class-E LCCL CPT system designed for high-frequency operation at 1 MHz with a 24 V dc supply and a 50 Ω load. The Class-E resonant inverter is used to reduce switching loss through zero-voltage switching (ZVS), whereas the LCCL compensation network is introduced to improve impedance matching across the capacitive coupler. The prototype was evaluated at a nominal plate separation of 1 mm and compared with MATLAB/Simulink results. Simulation produced 98.28% efficiency, while experimental validation achieved 96.25% efficiency with approximately 10 W delivered to the load. A plate-gap study from 1 mm to 10 mm shows that efficiency decreases from 95.45% to 72.06% as the coupling capacitance weakens. The results verify that the Class-E LCCL topology is suitable for compact low-power CPT applications, especially where metallic surroundings, simple coupler structure, and reduced magnetic-field effects are important.**

Index Terms—Capacitive power transfer, Class-E inverter, impedance matching, LCCL compensation, low-power wireless charging, zero-voltage switching.

I. INTRODUCTION

Wireless power transfer (WPT) removes the conductive link between source and load, thereby reducing connector wear, improving user safety, and enabling sealed or moving systems to be powered without exposed terminals. Inductive power transfer (IPT) has been widely adopted in consumer electronics and electric vehicle charging, but its reliance on magnetic coupling makes it sensitive to metallic surroundings, eddy-current heating, and bulky magnetic materials. Capacitive power transfer (CPT), by contrast, uses an alternating electric field between conductive plates and can be implemented with flat, low-cost electrodes.

Recent reviews and high-impact journal papers show that CPT has progressed from low-power demonstrations to kilowatt-level electric vehicle chargers, largely through improved coupler geometry, compensation networks, and high-frequency power converters [6]-[12]. JEESR literature also confirms the relevance of resonant converters, impedance matching, power electronic modelling, and low-power biomedical circuits to the local electrical and electronic systems research community [1]-[5]. This motivates a compact CPT design that can be experimentally validated using accessible components while still being positioned against current Scopus-indexed WPT literature.

The main limitation of CPT is that the coupling capacitance depends strongly on plate area, dielectric permittivity, and separation distance. Small gap variations shift the reflected impedance and may disrupt the intended ZVS condition. For this reason, a suitable compensation network is needed between the Class-E inverter and the capacitive coupler. In this work, a Class-E LCCL topology is investigated because it combines high-frequency switching capability, harmonic attenuation, and impedance transformation in a single compact structure.

The contributions of this paper are threefold. First, the thesis-scale Class-E LCCL CPT prototype is reformulated into a journal-ready technical article. Second, the design is strengthened with recent JEESR and Scopus Q1/Q2 literature on CPT, WPT, high-frequency converters, and energy-harvesting systems. Third, the experimental results are discussed using a more critical Q2-style research narrative that highlights ZVS validity, simulation-experiment deviation, and plate-gap sensitivity.

II. RELATED WORK AND JOURNAL POSITIONING

A. Capacitive Wireless Power Transfer

CPT transfers energy through electric-field coupling between transmitter and receiver plates. For an ideal parallel plate approximation, the coupling capacitance can be described by $C = \varepsilon_0 \varepsilon_r A/d$, where A is the effective plate area and d is the

This manuscript is submitted on May 29, 2026, revised on July 29, 2026, accepted on July 30, 2026, and published on October 31, 2026.

Muhammad Izzat Ariff Bin Sulaiman, Khairul Kamarudin Bin Hasan*, Nor Diyana Binti Md Sin, Zakariah Bin Yusuf, Siti Aminah Nordin are with Faculty of Electrical Engineering, Universiti Teknologi MARA Johor Branch Campus.

*Corresponding author
Email address: khairul@uitm.edu.my

1985-5389/© 2026 The Authors. Published by UiTM Press. This is an open access article under the CC BY-NC-ND license (http://creativecommons.org/licenses/by-nc-nd/4.0/).

separation distance. This relationship explains why the delivered output power and efficiency drop as the plate gap increases. It also explains why high-power CPT systems require either large plates, dielectric enhancement, high switching frequency, or advanced compensation circuits.

Lu et al. reviewed the development of CPT technology and emphasized compensation topology and coupler design as the two dominant factors governing power density and efficiency [6]. Erel et al. later expanded this view by classifying CPT fundamentals, component technologies, applications, and limitations in a comprehensive IEEE Access review [7]. These works provide the broader Q1/Q2 journal foundation for the present low-power prototype.

B. Class-E and Compensation Networks

The Class-E inverter is attractive for MHz-range CPT because it can operate with low switching loss when ZVS is satisfied. The switching device turns on when the drain-to-source voltage approaches zero, allowing the energy stored in the switch capacitance to be recovered instead of dissipated. The classical Class-E principle originates from the tuned single-ended switching amplifier introduced by Sokal and Sokal [20].

In CPT systems, the inverter does not operate in isolation. The capacitive coupler presents a small and distance-dependent capacitance, so the load seen by the inverter can deviate from the desired operating point. Independent CPT studies and reviews have established that compensation design, coupler variation, and the preservation of zero-voltage switching are central to efficient high-frequency operation [6], [7], [18]. These findings support the use of a Class-E LCCL network in the present work.

C. Relevance of JEESR Literature

Five JEESR papers were used to strengthen the local journal positioning of this manuscript. Nuawi et al. demonstrated the design of a MOSFET-based high-frequency resonant charging circuit [1], while Ismail and Abd Kadir showed the importance of matching impedance in RF-to-dc energy-harvesting rectifiers [2]. Ghazali et al. modelled a multi-input single-output power supply using a single-phase matrix converter, demonstrating the relevance of converter-level simulation in JEESR [3]. Karim reported a low-power readout circuit for biomedical MEMS applications [4], and Zainal Abidin et al. reviewed piezoelectric energy harvesting for low-power systems [5]. Together, these works support the journal fit of resonant conversion, impedance matching, energy transfer, and low-power application themes.

III. System Design And Methodology

A. System Architecture

The proposed system consists of a dc supply, a single-ended Class-E MOSFET inverter, an LCCL compensation network, a four-plate capacitive coupler, and a resistive load. The inverter converts the 24 V dc input into a high-frequency ac excitation at 1 MHz. The LCCL network transforms the small capacitive-coupler impedance into a more suitable load condition for the Class-E stage while filtering unwanted harmonics.

The coupler uses a bipolar plate arrangement because it provides a clearer return-current path and stronger coupling than a single-pair unipolar arrangement. The nominal separation distance is fixed at 1 mm for the main design point. The output is evaluated across a 50 Ω load, which represents a low-power charging or auxiliary supply condition.

Key design parameters are Vcc = 24 V, f = 1 MHz, Lchoke = 230 µH, C1 = 879.524 pF, L1 = 52.877 µH, Cp = 120.85 pF, C2 = 474.142 pF, C3 = 608.55 pF, L3 = 40.04 µH, and RL = 50 Ω. These values define the nominal Class-E LCCL operating point used in both simulation and hardware testing.

B. Circuit Configuration and Operating Principle

Fig. 1 shows the complete Class-E LCCL CPT circuit used as the basis of both the simulation model and the hardware implementation. The left-hand side is the transmitter unit, which consists of the dc input source, the single-ended Class-E switching stage, the choke inductor, and the transmitter-side LCCL compensation network. This stage converts the 24 V dc supply into a 1 MHz high-frequency excitation while maintaining the zero-voltage switching (ZVS) condition required for high-efficiency operation.

The middle section represents the capacitive coupling interface. A bipolar plate arrangement is used so that one plate pair provides the forward displacement-current path and the other provides the return path. These capacitive plates act as the wireless coupling medium, and their equivalent coupling capacitance varies with plate area, dielectric properties, and plate separation. Because this coupling capacitance is relatively small, the matching network is essential to transform the effective load and to sustain efficient power transfer across the air gap.

On the right-hand side, the receiver unit contains the receiver-side compensation elements, rectified/measured output path, and the 50 Ω resistive load used during validation. The receiver network resonates with the coupling capacitance and improves impedance matching between the transmitter and the load. As a result, the overall system suppresses excessive reactive power circulation, improves power-delivery capability, and preserves the expected Class-E operating waveforms. This circuit-level arrangement therefore explains why the prototype can achieve high efficiency at the nominal 1 mm plate spacing.

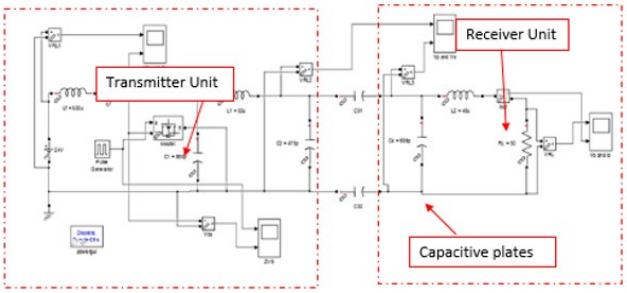


Fig. 1. Complete circuit configuration of the proposed Class-E LCCL capacitive power transfer system, showing the transmitter unit, receiver unit, and capacitive coupling plates.

C. Experimental Procedure

The circuit in Fig. 1 was first evaluated in simulation to

verify ZVS operation, voltage and current stress, and power-transfer efficiency. The hardware prototype was then assembled and tested under the same nominal design conditions to enable direct comparison between simulated and experimental performance. The experimental setup used for this validation is shown in Fig. 2.

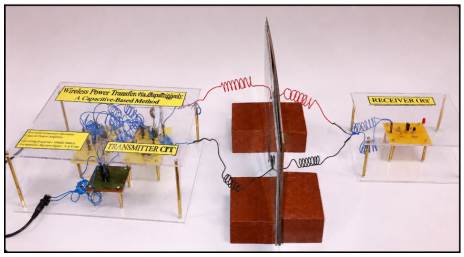


Fig. 2. Experimental setup of the Class-E LCCL CPT prototype showing the transmitter circuit, capacitive plates, receiver unit, and measurement instruments.

The experimental layout separates the transmitter and receiver by the capacitive plate interface, allowing the output voltage and current to be measured without a direct conductive connection. The visible 1 mm plate spacing is important because the LCCL component values were selected for this nominal coupling capacitance. Any physical movement of the plates changes the reflected impedance and therefore affects both output power and ZVS robustness.

Efficiency was calculated using $\eta = (P_{out}/P_{in}) \times 100\%$, where Pin is the dc input power and Pout is the rms output power delivered to the 50 Ω loads. The present hardware validation used this single nominal load to isolate the effect of plate separation. After verifying the 1 mm nominal point, the plate separation varied from 1 mm to 10 mm to evaluate coupling sensitivity.

IV. Results And Discussion

A. Zero-Voltage Switching Performance

Fig. 3 compares the simulated and measured ZVS behaviour. The simulated drain-to-source voltage was 87.77 V with a 10 V gate signal, while the experimental drain-to-source voltage increased to approximately 97 V with a 17 V gate signal. In both cases, the drain voltage reached near zero before turn-on, confirming that the ZVS condition was preserved.

The observed drain voltage is approximately three to four times the dc input voltage, which agrees with conventional Class-E waveform behavior. This is important because the main objective of the LCCL network is not only to deliver power through the capacitive coupler but also to preserve Class-E switching conditions under the selected load and gap.

The experimental waveform confirms the same switching trend as the simulation, although the measured peak drain voltage is higher. This increase is mainly attributed to parasitic inductance in the wiring and PCB path, tolerance of the resonant capacitors and inductors, and oscilloscope probe effects. More importantly, the valley of the drain-to-source voltage still occurs before the gate pulse turns the MOSFET on. Therefore, the deviation does not invalidate the Class-E design; instead, it shows that the prototype maintains soft-switching behaviour under realistic hardware conditions.

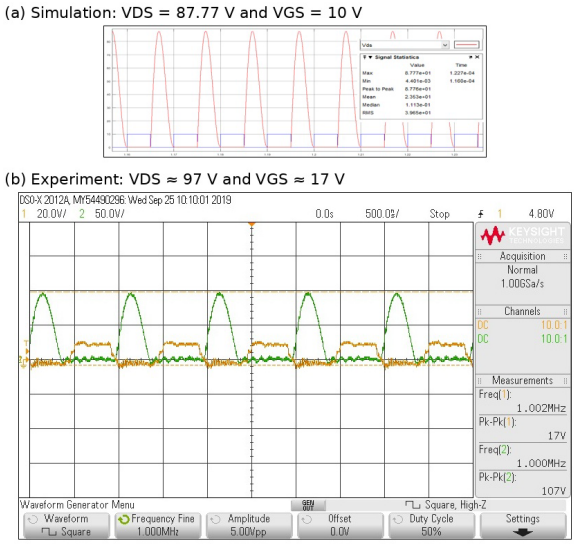


Fig. 3. ZVS waveform comparison for the Class-E LCCL CPT system: (a) simulation and (b) experimental oscilloscope measurement.

B. Input-Output Power and Efficiency

The nominal design parameters listed in Section III-A were used for both the simulation and hardware comparison.

The simulation-experiment comparison presented in Figs. 4 until 6 demonstrates a close agreement between the simulated model and the hardware prototype at the nominal plate separation of 1 mm. At this operating point, the Class-E LCCL CPT system successfully maintained stable power transfer under the intended 24 V dc supply and 1 MHz switching frequency. The simulated efficiency of 98.28% and the experimentally measured efficiency of 96.25% indicate that the selected component values, compensation network, and impedance matching approach are appropriate for a 10 W low-power capacitive wireless power transfer application.

The relatively small efficiency difference of approximately 2.03 percentage points confirms that the practical prototype follows the expected behaviour of the simulation model. This result suggests that the LCCL compensation network can transform the capacitive coupling interface into a suitable load condition for the Class-E inverter. In addition, the close efficiency agreement verifies that the transmitter-side and receiver-side compensation elements are properly tuned to support effective energy transfer across the capacitive plates while preserving the desired resonant operation.

Nevertheless, the measured efficiency is slightly lower than the simulated value because several non-ideal factors are unavoidable in the experimental setup. These include parasitic resistance in the circuit conductors, non-ideal MOSFET output capacitance, equivalent series resistance of the inductors and capacitors, probe loading during oscilloscope measurement, and stray impedance introduced by the physical wiring layout. Since these practical losses are not fully represented in the idealised simulation model, the observed reduction in

efficiency is considered acceptable for a 1 MHz laboratory-scale prototype. Overall, the result validates the feasibility of the proposed Class-E LCCL CPT system for efficient low-power wireless charging at short coupling distance.

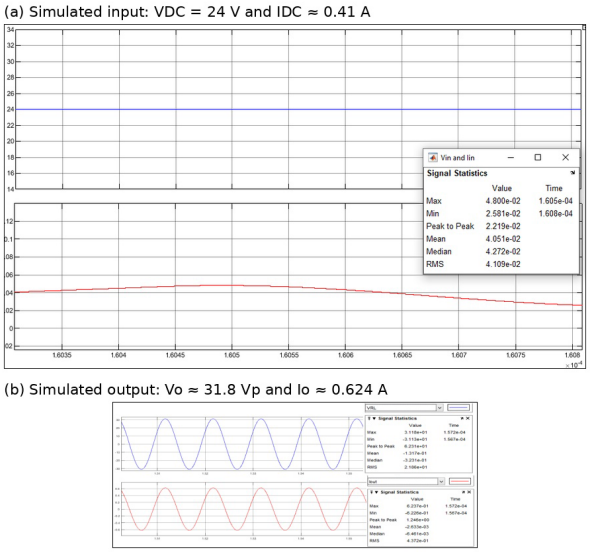


Fig. 4. Simulated input and output waveforms of the Class-E LCCL CPT system at 24 V dc supply and 1 MHz switching frequency.

The simulated waveforms show that the dc input remains stable at 24 V while the output voltage and current are approximately sinusoidal at the receiver side. This behaviour indicates that the LCCL network does not only perform impedance transformation but also filters high-frequency harmonics generated by the switching stage. The sinusoidal receiver waveform is a useful indicator that the load is being driven through the intended resonant path rather than through uncontrolled parasitic coupling.

Compared with high-power EV-oriented CPT systems, the present prototype targets a smaller and safer low-power range. However, the achieved efficiency is competitive for short-range CPT and confirms that a simple four-plate structure can deliver stable power when the operating point is tightly controlled.

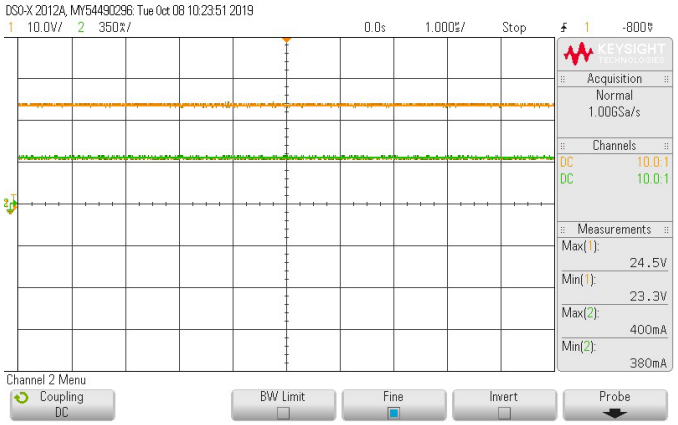


Fig. 5. Experimental input measurement showing approximately 24 V dc input voltage and 0.40 A input current at the nominal 1 mm plate distance.

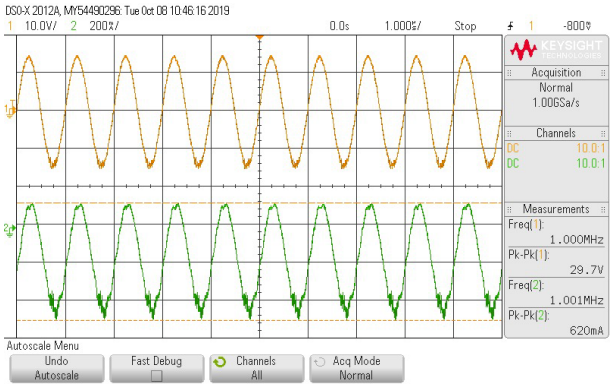


Fig. 6. Experimental receiver-side output voltage and current waveforms showing 1 MHz operation and approximately 29.7 V peak output voltage.

Figures 5 and 6 verify the measured power-transfer path from the dc supply to the receiver load. The input measurement gives an input power close to 9.6 W, while the reported 96.25% efficiency corresponds to an output power of approximately 9.24 W, which is close to the 10 W design target. The output current trace contains small waveform distortion near the negative valley, which is consistent with non-ideal rectification, probe grounding, and parasitic coupling around the receiver network. Nevertheless, the measured output waveform remains periodic at approximately 1 MHz, confirming that the hardware prototype follows the simulated resonant operating mode.

All measurements reported in this subsection were obtained at the nominal 50 Ω resistive load. Accordingly, the efficiency and waveform agreement demonstrate validity at the design point only and should not be interpreted as evidence of load-invariant performance. A complete practical validation should include at least three representative load levels spanning light, nominal, and heavy loading, with output power, efficiency, and ZVS retention evaluated at each condition.

C. Effect of Plate Separation

The plate-gap study used the nominal parameters defined in Section III-A, with only the plate separation varied.

The plate-gap analysis confirms that the proposed system is highly optimized for a 1 mm coupling distance. As the gap increases, the coupling capacitance decreases and the impedance seen by the Class-E inverter departs from its matched condition. Consequently, the input power rises slightly while the output power declines, indicating increased reactive circulation and reduced real power transfer.

The efficiency degradation from 95.45% at 1 mm to 72.06% at 10 mm highlights the need for future adaptive tuning if the system is intended for misalignment-tolerant or dynamic applications. The experimental setup in Fig. 1 also explains this sensitivity: because the coupling interface is physically small and air-spaced, even a few millimetres of plate displacement reduce coupling capacitance and move the reflected load away from the optimum Class-E LCCL design point. Recent Q1/Q2 CPT studies address this issue using shielded couplers, high-order compensation, frequency tuning, and multi-MHz

operation [10], [14], [18], [19].

D. Comparative Positioning

In relation to CPT review papers [6], [7], [16], [17], this prototype demonstrates a smaller fixed-gap implementation rather than a generalized coupler or control framework. Compared with high-power EV-oriented work [8]-[11], [19], the proposed hardware is lower in power but simpler in structure and suitable for laboratory replication. The Class-E and ZVS aspects are aligned with established switching-amplifier theory [20] and independent CPT studies on compensation, coupler design, and soft-switching operation [6], [7], [18].

The novelty of this article does not rely on proposing an entirely new capacitive power transfer (CPT) compensation topology. Instead, its contribution is the systematic design, simulation, hardware validation, and critical positioning of a compact Class-E LCCL CPT prototype developed from earlier project work [22]. The prototype is presented as a reproducible engineering platform, with emphasis on impedance matching, zero-voltage switching operation, simulation-experiment deviation, and plate-gap sensitivity.

From an application perspective, the proposed system provides a practical low-power CPT platform that can be further developed for several compact wireless power applications. The successful operation at 24 V dc, 1 MHz switching frequency, and 1 mm plate separation shows that the Class-E LCCL configuration is suitable for short-range energy transfer where physical connectors are undesirable. This makes the system relevant to biomedical charging, sealed electronic devices, low-power sensor nodes, and compact auxiliary power supplies. Although the present prototype is limited to a fixed coupling distance, its high measured efficiency confirms that the selected circuit parameters and compensation network can support reliable wireless energy transfer under controlled operating conditions.

The study also identifies an important direction for future technical improvement. Since the experimental results show that efficiency decreases when the plate gap increases, future work should focus on closed-loop frequency tuning or adaptive impedance matching. Such a control strategy would allow the system to maintain the desired zero-voltage switching condition even when the coupling capacitance changes due to plate displacement, gap variation, or load fluctuation. Therefore, the next stage of development should move beyond fixed-frequency operation toward a more robust and adaptive Class-E LCCL CPT system capable of preserving both efficiency and switching performance under practical operating conditions.

V. Conclusion

A Class-E LCCL capacitive wireless power transfer system for low-power charging applications has been designed, simulated, and experimentally validated. At 24 V dc input, 1 MHz switching frequency, 50 Ω load, and 1 mm plate separation, the prototype delivered approximately 10 W with 96.25% measured efficiency, close to the 98.28% simulation result. The ZVS waveform confirms that the Class-E inverter and LCCL network operate as intended at the nominal design point. The plate-separation analysis confirms that the proposed Class-E LCCL CPT system is strongly dependent on coupling distance. At the nominal 1 mm plate separation, the system operates near its optimum design condition and achieves high power-transfer efficiency. However, as the plate gap increases, the coupling capacitance decreases, causing the reflected load impedance seen by the Class-E inverter to deviate from the intended matching condition. This effect becomes more significant at larger gaps, where the efficiency drops to 72.06% at 10 mm.

This reduction in efficiency indicates that the present design is most suitable for fixed short-range low-power CPT applications, where the plate distance can be maintained accurately. Under this condition, the LCCL compensation network can provide effective impedance matching and support stable resonant operation. However, for applications involving movement, vibration, misalignment, or variable air gaps, the fixed-frequency and fixed-component design may not be sufficient to preserve optimum performance. Therefore, the system would require additional control or compensation strategies to maintain zero-voltage switching and reduce power loss under changing coupling conditions.

Future work should therefore focus on improving the robustness and practical safety of the system. Electric-field simulation should be conducted to analyse field distribution around the capacitive plates and to verify compliance with applicable human-exposure limits [21]. Thermal analysis is also required to evaluate heating effects in the MOSFET, inductors, capacitors, and coupling structure during continuous operation. In addition, hardware testing should be extended to at least three representative load conditions, followed by adaptive frequency tuning or closed-loop impedance matching to compensate for changes in plate separation and load. These improvements would allow the Class-E LCCL CPT system to operate more reliably in practical low-power wireless charging applications while maintaining efficiency, safety, and stable switching performance.

Acknowledgement

The authors acknowledge the Faculty of Electrical Engineering, Universiti Teknologi MARA Johor Branch, Pasir Gudang Campus, Malaysia, for the technical support, facilities, and resources provided during the prototype development and experimental testing stages.

References

[1] N. A. A. Nuawi, E. A. Kadir, and M. N. Seroji, "A 120 kHz high-frequency MOSFET charging circuit using series parallel resonant converter," Journal of Electrical and Electronic Systems Research, vol. 21, no. 1, 2022, doi: 10.24191/jeesr.v21i1.001.

[2] N. Ismail and E. A. Kadir, "Reversed L-type matching impedance of RF-to-DC rectifier for energy harvesting system," Journal of Electrical and Electronic Systems Research, vol. 19, no. 1, pp. 167-172, 2021, doi: 10.24191/jeesr.v19i1.022.

[3] M. S. M. Ghazali, M. Z. M. Zaki, R. Baharom, N. H. Abdullah, and M. S. M. Rawi, "Modelling and simulation of multi-input single-output DC power supply using single phase matrix converter (SPMC)," Journal of Electrical and Electronic Systems Research, vol. 19, no. 1, pp. 117-124,

2021, doi: 10.24191/jeesr.v19i1.015.

[4] J. Karim, "Low-power current-mode resistive readout circuit using 0.13 µm technology for biomedical MEMS applications," Journal of Electrical and Electronic Systems Research, vol. 26, no. 1, pp. 57-63, 2025, doi: 10.24191/jeesr.v26i1.007.

[5] N. A. K. Zainal Abidin, N. Mohd Nayan, N. Jamel, and A. Ali, "A review of piezoelectric energy harvesting in shape and array configuration," Journal of Electrical and Electronic Systems Research, vol. 25, no. 1, pp. 1-12, 2024, doi: 10.24191/jeesr.v25i1.001.

[6] F. Lu, H. Zhang, and C. C. Mi, "A review on the recent development of capacitive wireless power transfer technology," Energies, vol. 10, no. 11, p. 1752, 2017, doi: 10.3390/en10111752.

[7] M. Z. Erel, K. C. Bayindir, M. T. Aydemir, S. K. Chaudhary, and J. M. Guerrero, "A comprehensive review on wireless capacitive power transfer technology: Fundamentals and applications," IEEE Access, vol. 10, pp. 3116-3143, 2022, doi: 10.1109/ACCESS.2021.3139761.

[8] J. Dai and D. C. Ludois, "Capacitive power transfer through a conformal bumper for electric vehicle charging," IEEE Journal of Emerging and Selected Topics in Power Electronics, vol. 4, no. 3, pp. 1015-1025, Sep. 2016, doi: 10.1109/JESTPE.2015.2505622.

[9] F. Lu, H. Zhang, H. Hofmann, and C. C. Mi, "A double-sided LCLC-compensated capacitive power transfer system for electric vehicle charging," IEEE Transactions on Power Electronics, vol. 30, no. 11, pp. 6011-6014, Nov. 2015, doi: 10.1109/TPEL.2015.2446891.

[10] H. Zhang, F. Lu, H. Hofmann, W. Liu, and C. C. Mi, "Six-plate capacitive coupler to reduce electric field emission in large air-gap capacitive power transfer," IEEE Transactions on Power Electronics, vol. 33, no. 1, pp. 665-675, Jan. 2018, doi: 10.1109/TPEL.2017.2662583.

[11] F. Lu, H. Zhang, H. Hofmann, and C. C. Mi, "A double-sided LC-compensation circuit for loosely coupled capacitive power transfer," IEEE Transactions on Power Electronics, vol. 33, no. 2, pp. 1633-1643, Feb. 2018, doi: 10.1109/TPEL.2017.2674682.

[12] S. Li and C. C. Mi, "Wireless power transfer for electric vehicle applications," IEEE Journal of Emerging and Selected Topics in Power Electronics, vol. 3, no. 1, pp. 4-17, Mar. 2015, doi: 10.1109/JESTPE.2014.2319453.

[13] G. A. Covic and J. T. Boys, "Modern trends in inductive power transfer for transportation applications," IEEE Journal of Emerging and Selected Topics in Power Electronics, vol. 1, no. 1, pp. 28-41, Mar. 2013, doi: 10.1109/JESTPE.2013.2264473.

[14] M. Tamura, Y. Naka, K. Murai, and T. Nakata, "Design of a capacitive wireless power transfer system for operation in fresh water," IEEE Transactions on Microwave Theory and Techniques, vol. 66, no. 12, pp. 5873-5884, Dec. 2018.

[15] B. Minnaert and N. Stevens, "Optimal analytical solution for a capacitive wireless power transfer system with one transmitter and two receivers," Energies, vol. 10, no. 9, p. 1444, 2017, doi: 10.3390/en10091444.

[16] J. Zhang, Y. Zhao, X. Zhang, and Y. Li, "A review of capacitive power transfer technology for electric vehicle wireless charging," Electronics, vol. 12, no. 16, p. 3534, 2023.

[17] Z. Wang, Y. Zhang, and X. Li, "Research and application of capacitive power transfer technology," Electronics, vol. 11, no. 7, p. 1158, 2022.

[18] F. Corti, A. Reatti, and G. Grasso, "Zero voltage switching condition in Class-E inverter for capacitive wireless power transfer applications," Energies, vol. 14, no. 4, p. 911, 2021, doi: 10.3390/en14040911.

[19] E. Rong, P. Sun, and G. Yang, "5-kW, 96.5% efficiency capacitive power transfer system with a five-plate coupler: Design and optimization," IEEE Transactions on Power Electronics, vol. 40, no. 1, pp. 2542-2555, Jan. 2025, doi: 10.1109/TPEL.2024.3462410.

[20] N. O. Sokal and A. D. Sokal, "Class E - A new class of high-efficiency tuned single-ended switching power amplifiers," IEEE Journal of Solid-State Circuits, vol. 10, no. 3, pp. 168-176, Jun. 1975, doi: 10.1109/JSSC.1975.1050582.

[21] International Commission on Non-Ionizing Radiation Protection, "Guidelines for limiting exposure to time-varying electric, magnetic and electromagnetic fields (up to 300 GHz)," Health Physics, vol. 74, no. 4, pp. 494-522, 1998.

[22] M. I. A. Sulaiman, "Class-E LCCL capacitive wireless power transfer for low power consumption," Final Year Project Report, Universiti Teknologi MARA, Malaysia, 2021.